



Methylglyoxal-Mediated Dopamine Depletion, Working Memory Deficit, and Depression-Like Behavior Are Prevented by a Dopamine/Noradrenaline Reuptake Inhibitor

Gudrian Ricardo Lopes de Almeida¹ · Jozimar Carlos Szczepanik² · Ingrid Selhorst³ · Ariana Ern Schmitz³ · Bárbara dos Santos³ · Maurício Peña Cunha¹ · Isabella Aparecida Heinrich² · Gabriela Cristina de Paula³ · Andreza Fabro De Bem^{1,4} · Rodrigo Bairy Leal^{1,2,3} · Alcir Luiz Dafre^{1,2,3}

Received: 27 April 2020 / Accepted: 22 September 2020 / Published online: 4 October 2020
© Springer Science+Business Media, LLC, part of Springer Nature 2020

Abstract

Methylglyoxal (MGO) is an endogenous toxin, mainly produced as a by-product of glycolysis that has been associated to aging, Alzheimer's disease, and inflammation. Cell culture studies reported that MGO could impair the glyoxalase, thioredoxin, and glutathione systems. Thus, we investigated the effect of in vivo MGO administration on these systems, but no major changes were observed in the glyoxalase, thioredoxin, and glutathione systems, as evaluated in the prefrontal cortex and the hippocampus of mice. A previous study from our group indicated that MGO administration produced learning/memory deficits and depression-like behavior. Confirming these findings, the tail suspension test indicated that MGO treatment for 7 days leads to depression-like behavior in three different mice strains. MGO treatment for 12 days induced working memory impairment, as evaluated in the Y maze spontaneous alternation test, which was paralleled by low dopamine and serotonin levels in the cerebral cortex. Increased DARPP32 Thr75/Thr34 phosphorylation ratio was observed, suggesting a suppression of phosphatase 1 inhibition, which may be involved in behavioral responses to MGO. Co-treatment with a dopamine/noradrenaline reuptake inhibitor (bupropion, 10 mg/kg, p.o.) reversed the depression-like behavior and working memory impairment and restored the serotonin and dopamine levels in the cerebral cortex. Overall, the cerebral cortex monoaminergic system appears to be a preferential target of MGO toxicity, a new potential therapeutic target that remains to be addressed.

Keywords Methylglyoxal · Mood disorder · Working memory · Dopamine · DARPP32

Abbreviations

5-HT Serotonin
AGE Advanced glycation end products

AKR Aldo-keto reductase
BUP Bupropion
Ctl Control
DA Dopamine
DARPP32 Dopamine and cAMP-regulated phosphoprotein of 32 kDa
D J 1 / PARK7 Protein deglycase 1/Parkinsonism-associated deglycase
GCL Glutamate-cysteine ligase
Glo Glyoxalase
GR Glutathione reductase
GSH Glutathione
HP Hippocampus
MGO Methylglyoxal
NE Norepinephrine
OLT Object location task
PFC Prefrontal cortex
TH Tyrosine hydroxylase

Electronic supplementary material The online version of this article (<https://doi.org/10.1007/s12035-020-02146-3>) contains supplementary material, which is available to authorized users.

✉ Alcir Luiz Dafre
alcir.dafre@ufsc.br

¹ Biochemistry Post-Graduation Program, Federal University of Santa Catarina, Florianópolis, SC 88040-900, Brazil

² Neurosciences Post-Graduation Program, Federal University of Santa Catarina, Florianópolis, SC 88040-900, Brazil

³ Department of Biochemistry, Biological Sciences Center, Federal University of Santa Catarina, Florianópolis, SC 88040-900, Brazil

⁴ Department of Physiological Science, Institute for Biological Sciences, University of Brasília, Brasília, Brazil

Trx	Thioredoxin
TrxR	Thioredoxin reductase
TST	Tail suspension test

Introduction

Methylglyoxal (MGO) is an endogenous by-product in normal metabolism of carbohydrates, lipids, and proteins, inevitably produced spontaneously or enzymatically [1]. Accumulation of MGO is highly deleterious as it readily reacts in vivo with basic phospholipids and nucleotides and with lysine, arginine, and cysteine residues of proteins, leading to formation of advanced glycation end products (AGEs). MGO has been proposed to contribute in a number of pathologies, such as diabetes, inflammation, and Alzheimer's disease [2]. Disturbances in MGO metabolism, increasing MGO serum levels, can be found in elderly and have been associated with increased cognitive decline [3]. Alzheimer's and diabetic patients also present elevated levels of MGO in the cerebrospinal fluid and increased formation of AGEs [4], suggesting MGO is a major factor in the development of these pathologies [5].

The glyoxalase system is the main enzymatic route for MGO detoxification, as lowering of glyoxalase 1 (Glo1) activity may contribute to increasing MGO levels [4]. There are other enzymatic routes capable of reducing α -oxoaldehydes such as MGO, including aldo-keto reductases (AKRs) and protein deglycase 1/Parkinsonism-associated deglycase (DJ1/PARK7), proteins known to catalyze the oxidation and reduction of carbonyl groups depending on NADPH as an electron donor [6]. The deglycase activity, and the ability to repair glycated proteins, like α -synuclein, indicates the DJ1 potential relevance to neurodegenerative diseases [7–9].

Prior to enzymatic attack, MGO reacts spontaneously with glutathione (GSH), generating hemithioacetal, a substrate for Glo1. The product of Glo1 catalysis, *S*-D-lactoylglutathione, is a substrate for glyoxalase 2 (Glo2), regenerating GSH and resulting in the formation of D-lactate, terminating the cycle [10]. It has been demonstrated that, shortly after MGO exposure, GSH levels are decreased by reacting with MGO [10]. It has also been shown that MGO can impair the glyoxalase system by decreasing Glo2 protein in HT22 cells [11], in an AMPK-dependent autophagy process [12]. Thus, MGO itself can induce weakening of the glyoxalase system, favoring MGO accumulation.

Disturbances in the glyoxalase [13] and redox systems [14] are connected to several pathological conditions; therefore, assessing the status of these cellular defenses may contribute to the understanding of MGO toxicity. In alleviating oxidative damage to biomolecules, the redox capacity is substantially dependent on reducing systems, such as GSH/glutathione reductase (GR) and thioredoxin (Trx)/thioredoxin reductase (TrxR). Both reductases use the reducing equivalents

provided by NADPH. GR reduces oxidized glutathione [15], while TrxR maintains Trx in its reduced and active form [16]. Interestingly, the Trx and GSH systems have been indicated as molecular targets of MGO in HT22 nerve cells [11]. These and other data suggest that MGO is potentially detrimental to the cellular antioxidant protection.

Diabetic patients and rats present elevated plasma levels of MGO [17, 18], and higher MGO levels are positively associated with poorer memory and executive function and a faster rate of cognitive decline [3, 19]. The evidences in animal studies indicating that MGO is associated to cognitive impairment are limited, highlighting the need for further investigation [20, 21].

Changes in Glo1 expression, or in the levels of MGO, were associated with the anxiety, seizure, pain, and depression-like behavior in mice [21–27]. Although limited data are available, some studies indicate an involvement of MGO, or alterations in Glo1 expression, in generating depression-like behavior. Studies are controversial, some studies indicate MGO presents an antidepressant effect, but others indicate MGO is depressogenic [21, 28–31].

A previous work of our group demonstrated that MGO treatment depleted dopamine (DA) in the prefrontal cortex (PFC) and induced memory deficits and depression-like behavior in female mice [21]. DA reuptake inhibitors, such as bupropion (BUP), are commonly used drugs for treating major depression disorder [32] and producing antidepressant-like effects in rodents [33, 34]. Furthermore, the administration of BUP abrogated the scopolamine-induced memory impairment [35], suggesting BUP can be a good candidate for alleviating these MGO deleterious effects.

Given in vitro literature data indicating that the Glo, Trx, and GSH systems would be targeted by MGO [11, 12, 36], elements of these systems were investigated in the PFC and hippocampus (HP) of mice treated with MGO. The importance of the dopaminergic system in the pathophysiology and treatment of depression, and in memory and learning deficits, prompted us to investigate whether the dopaminergic transmission was impaired by MGO, as evaluated by DA levels and dopamine and cAMP-regulated phosphoprotein of 32 kDa (DARPP32) phosphorylation. Based on the fact that MGO can deplete DA in the cerebral cortex of mice [21], we investigated if BUP can prevent memory deficits, depression-like behavior, and depletion of monoamines induced by MGO.

Materials and Methods

Animals

Experiments were conducted using 3-month-old female mice. Swiss (35–50 g), C57BL/6 (20–26 g), or BALB/C (20–25 g)

strains were bred at the Federal University of Santa Catarina (UFSC), Florianópolis, Brazil. Mice were maintained at 21 °C ± 2 °C with free access to water and food, under a 12:12-h light/dark cycle (lights on at 07:00 hours). All manipulations were carried out between 09:00 and 17:00 hours. Mice were acclimatized to the experimental room for 2 h before the beginning of the tests. The experiments were performed in a dimly lit (20 lx) and sound-isolated room. The apparatus was cleaned with 10% ethanol between each mouse trial.

In a previous work, our group demonstrated that MGO treatment induced memory deficits and depression-like behavior in female mice [21]. Therefore, to keep pace with previous experimental conditions, female mice were used in this study. Furthermore, several studies have shown that the prevalence of stress-related psychiatric disorders (e.g., depression, post-traumatic stress disorder) is twice as prevalent in women compared to men [37], justifying the use of female mice.

The animal ethics committee of the Federal University of Santa Catarina (CEUA-UFSC, #7245210616) approved the experiments. All efforts were made to reduce the number of mice used and animal suffering, which is in conformity with the Guide for the Care and Use of Laboratory Animals, National Institutes of Health.

Experimental Protocol

Mice were treated with 0.9% saline (control) or 25 mg/kg or 50 mg/kg MGO dissolved in saline. Injections were performed by intraperitoneal (i.p.) route in a constant volume of 10 ml/kg of body weight.

Experiment 1

Mice received single daily doses of MGO (0 mg/kg, 25 mg/kg, or 50 mg/kg) during seven consecutive days (Fig. 1). Twenty-

four hours after the last MGO injection, mice were anesthetized with isoflurane, and killed by cervical dislocation. Prefrontal cortex (PFC) and hippocampus (HP) were collected for biochemical analyses.

Experiment 2

In another cohort of animals, mice were treated for 7 days, and the open field test and tail suspension test (TST) were performed 24 h after the last MGO injection (Fig. 1).

As we previously published, mice under MGO treatment developed depression-like behavior and memory impairments, accompanied with depletion of DA in the cerebral cortex [21]. In order to verify if BUP, a norepinephrine (NE) and DA reuptake inhibitor [32], could prevent these behavioral alterations, a third cohort of Swiss mice were tested in the experiment 3.

Experiment 3

To accommodate memory testing, saline, MGO, and MGO + BUP groups were treated for 11 days. This treatment protocol was successfully employed in a previous publication [21]. BUP (10 mg/kg) was administered by gavage 30 min prior to MGO (50 mg/kg) administration. On the 7th day, mice were tested on the Y-maze to assess spontaneous alternation, as a measure of working memory, and, on the 8th day, on the open field test and TST. On the 9th day, animals were exposed to the open field for habituation. On the 10th day, mice were placed once more for 10 min in the open field for training purpose, but now in the presence of two identical objects. On the 11th day, mice were placed in the open field for 5 min and one of the two identical objects was reallocated. Behavioral tests were performed 24 h after the last MGO injection. On the 12th day, mice were anesthetized with isoflurane and euthanized by

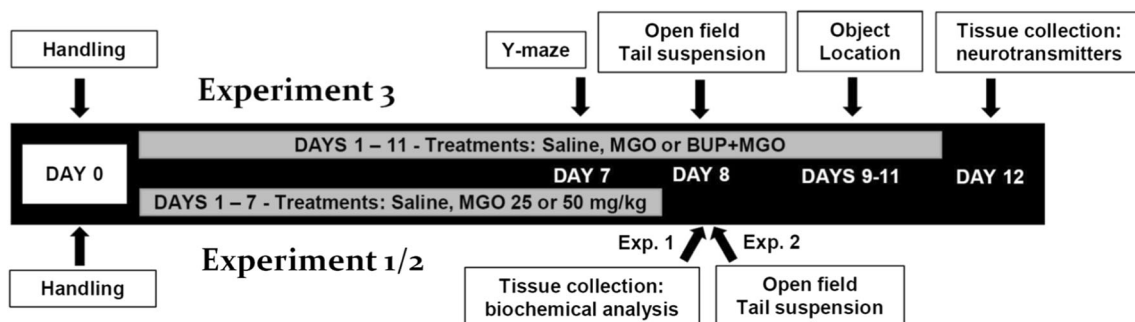


Fig. 1 Experimental design. Mice were treated for 7 days with MGO (0 mg/kg, 25 mg/kg, or 50 mg/kg), and 24 h later, the prefrontal cortex and hippocampus were collected (Exp. 1). An independent cohort of animals was submitted to the tail suspension test and exposed to the open field using three mice strains (Swiss, C57BL/6, and BALB/C; Exp. 2). A separate set of Swiss mice was submitted to MGO administration for 12 days. Three experimental groups were tested: control,

50 mg/kg MGO, i.p., or MGO in combination with BUP, 10 mg/kg, p.o. (Exp. 3). Mice were submitted to the Y-maze test on the 7th day, to the open field and tail suspension test on the 8th day, and to the object location task on the 11th day. Brain structures were collected 24 h after the behavioral test. BUP was applied in a daily basis, 30 min before MGO injection, and sample collection or behavioral tests were performed 24 h after the last MGO administration

cervical dislocation; PFC, HP, and striatum were collected for analyses of neurotransmitters.

Immunohistochemistry

Mice were anesthetized with isoflurane and perfused by transcardiac infusion of saline, followed by 4% paraformaldehyde. The brains were quickly removed, embedded in paraformaldehyde for 24 h, and cryoprotected by immersion in a 30% sucrose solution made in 0.1 M phosphate-buffered saline (PBS; pH 7.4), at 4 °C. Samples were frozen and stored at –80 °C until use. Serial frozen sections (20 µm) of hippocampi were cut on a cryostat (Leica) and collected on wells filled with PBS for free-floating immunohistochemistry.

For immunofluorescence analysis, prefrontal cortex and hippocampal slices were rinsed 3 times in 0.1 M PBS and blocked for 1 h by using blocking solution (PBS containing 5% horse serum (Gibco #16050122) and 0.5% Triton X-100 (Sigma-Aldrich) at 4 °C. Sections were incubated overnight at 4 °C with the antibody anti-MG-H1 (1:100; STA-011, Cell BioLabs, San Diego, USA) diluted in blocking solution. The sections were then subjected to three washes in 0.1 M PBS and incubated in the blocking solution for 2 h with anti-mouse Alexa 488 (Invitrogen, 1:400, A-11001), at room temperature. As a negative control, the primary antibody was omitted in order to demonstrate a lack of unspecific labeling (Supplementary Fig. S1). Sections were rinsed 3 times in 0.1 M PBS and mounted on gelatin-coated glass slides. Images were acquired on an Olympus IX83 microscopy, examined, and quantified using ImageJ software.

Biochemical Analysis

For t-GSH (the sum of reduced and oxidized GSH), the assay was performed by an enzymatic method [38]. Samples were homogenized in 0.5% perchloric acid at 1:10 (w/w) and centrifuged at 15,000g, for 5 min, and at 4 °C. Before assay, the supernatant was neutralized with 0.1 M potassium phosphate buffer and 1 mM ethylenediaminetetraacetic acid (pH 7.0). The obtained values were based on a standard curve made of GSH.

For enzymatic activity, samples were homogenized in 10 mM HEPES, 1.5 mM MgCl₂, 10 mM KCl, 0.5 mM dithiothreitol, 0.05% NP-40 with protease inhibitors (Sigma), and 1 mM PMSF (pH 7.2), at 1:10 (w/w), followed by sonication and centrifuged (20,000g, 15 min, 4 °C). Glo1 activity was measured in the supernatant, based on the *S*-lactoylglutathione formation, which can be monitored at 240 nm [39]. AKR activity was measured by NADPH reduction at 320 nm using MGO as the substrate [40].

The GR activity was measured based on the decrease in absorbance at 340 nm due to NADPH consumption, in the presence of oxidized GSH [15]. TrxR activity was measured

by the NADPH-dependent reduction of 5,5'-dithio-bis-(2-nitrobenzoic) acid, which was accompanied by the formation of 5'-thionitrobenzoic acid at 412 nm [16]. Protein in samples was quantified by the Bradford assay using bovine serum albumin as standard [41].

Western blotting of PFC and HP was performed in tissue samples first homogenized in ice-cold lysis buffer (50 mM Tris-HCl, pH 7.5, 150 mM NaCl, 1% NP-40, 1% protease inhibitor cocktail, 1 mM phenylmethylsulfonyl fluoride). Samples were subjected to SDS-PAGE electrophoresis, and proteins were electrotransferred to PVDF or nitrocellulose membranes and blocked with 5% non-fat powdered milk. Membranes were probed with the following primary antibodies: Glo1 (SC 67351, 1:1,000), Glo2 (SC 51092, 1:1,000), glutamate-cysteine ligase (GCL) (SC-22755, 1:3,000), and TrxR1 (SC 20147, 1:1,000) from Santa Cruz Biotechnology (Dallas, EUA). The antibody against the phosphorylated form of DARPP32 at Thr³⁴ (AB9206; 1:1,000) was from Millipore (Burlington, EUA). The antibody against GR (ab16801, 1:1,000) was from Abcam (Cambridge, UK). The antibody against DARPP32 (#2302, 1:1,000) and p-Thr⁷⁵-DARPP32 (#2301, 1:1,000; rabbit) were purchased from Cell Signaling (Danvers, USA). After incubation with the appropriate secondary antibody, ECL images were produced in a ChemiDoc apparatus (Bio-Rad, La Jolla) and quantified by ImageJ software (<https://imagej.nih.gov/ij/>). Band intensity was normalized to Ponceau S staining that produced a linear signal regarding protein load ($r^2 = 0.94$; $p < 0.0001$) in an experiment made in duplicate and gels loaded with 10, 20, 30, and 40 µg of protein (data not shown). For Ponceau S intensity measurements, the entire lane was used, but in figures, only a smaller area is presented.

Quantification of Neurotransmitters

Monoamine levels were determined by HPLC with fluorometric detection according to [42]. PFC, HP, and striatum of mice were homogenized in 0.2 M perchloric acid containing 3 mM cysteine at 1:5 (w/v). Homogenate was centrifuged (12,000×g, 10 min, 4 °C), and the resulting supernatant was frozen (–80 °C) for analysis. A standard curve was performed with concentrations ranging from 0.016 to 2.50 ng/µl and used to estimate the levels of DA, serotonin (5-HT), and NE. HPLC apparatus was from Jasco (LC-2000 Plus System), using an ACE[®] C18 Ultra-Inert column, at a flow rate of 0.6 ml/min. Monoamines were eluted in an isocratic solution of acetate (12 mM acetic acid, 0.26 mM ethylenediamine tetraacetic acid)/methanol (86:14, v/v) solution. The fluorescence was monitored using excitation at 279 nm and emission at 320 nm.

Behavior Tests

The immobility time was measured in the TST for 6 min, according to the method of Steru and collaborators [43]. Briefly, each animal was suspended by the tail for 6 min and at 60 cm above the ground. After the experimenter left the room, animal's behavior was recorded for 6 min, and the total immobility time was measured.

To exclude a possible interference, the locomotor activity was evaluated in the open field arena (40 cm × 40 cm × 30 cm). Briefly, each mouse was placed in the center of the arena to freely explore the apparatus for 5 min [44, 45]. The tests were recorded, and the distance traveled in the open field was subsequently analyzed using the ANY-Maze® software (Stoelting Co., Wood Dale, EUA).

Evaluation of working memory was carried out by measuring the spontaneous alternation rate of mice. When moving from one place to another, rodents exhibit the natural tendency to explore the least visited area or a previously known area which has changed (novelty), and this behavior is referred to as spontaneous alternation [46]. Spontaneous alternation was assessed using a Y-shaped maze, with three equal arms (30 cm × 10 cm × 25 cm height). Each mouse was placed in the center of the maze; then, during 5 min, the number of “correct” triplets (consecutive entries with all four paws in each of the three arms without re-entries) was registered and used as a measure of spontaneous alternation [47].

In order to evaluate long-term spatial memory, mice were submitted to the object location task (OLT), based on a protocol previously described [48, 49]. Briefly, 24 h after a habituation session for 5 min in the open field arena (40 cm × 40 cm × 30 cm), mice were placed again in the same arena for 10 min facing two identical objects (5 cm × 3 cm) for a training session. Long-term memory was evaluated 24 h after training, when one of the two objects was relocated and mice were re-exposed (test session). The time spent exploring the objects were recorded for 5 min. Visual cues were added in the test room as spatial reference.

Statistical Analysis

Pairwise comparisons were performed by Student's *t* test, while for multiple groups, one-way analysis of variance was used, followed by Dunnett's post hoc test. When failing to pass normality test, the Kruskal-Wallis analysis was employed, which was followed by Dunn's multiple comparisons test. OLT was analyzed using Student's *t* test by comparing the location index values to 50%. Values significantly higher than 50% implies that mice were able to discriminate the relocated object. The accepted level of statistical significance was $p < 0.05$. Data were expressed as mean + standard error of the mean (SEM), except when indicated.

Results and Discussion

The in vitro evidence showing that the glyoxalase, GSH, and Trx systems can be affected by MGO [11, 12, 36] prompted us to investigate the activity and relative protein content of enzymes in an in vivo model using typical components of these systems.

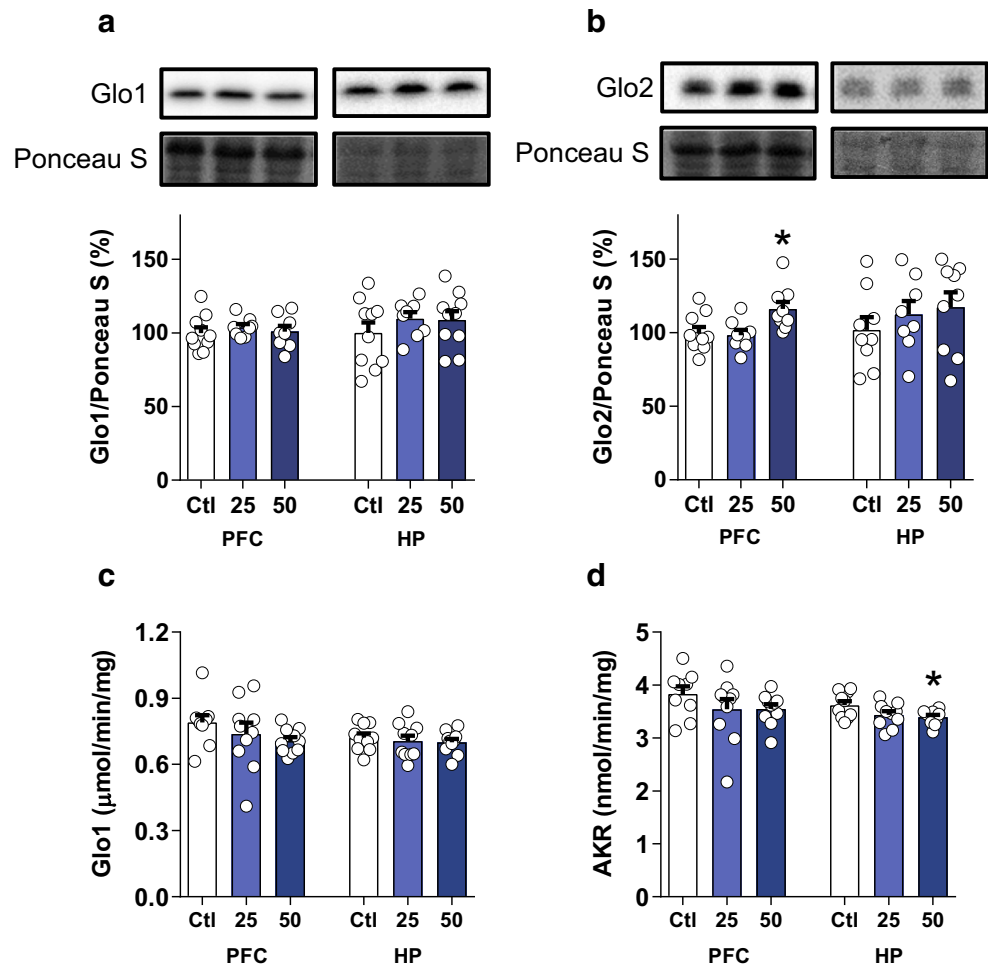
Glo1 is considered the first and limiting step in MGO detoxification; however, the Glo1 levels (Fig. 2a), and its enzyme activity (Fig. 2c), were not altered by MGO treatment. The second step in MGO detoxification depends on Glo2, and there are some evidences indicating the relevance of Glo2 in controlling MGO levels [50]. In this regard, a 16% increase in Glo2 protein levels in the PFC (Fig. 2b) may be understood as a compensatory response to MGO treatment, but confirmation remains to be produced. Overall, the glyoxalase system presented no major changes, indicating other compensatory mechanisms would have been induced.

Aldo-keto reductases have been shown to compensate for MGO detoxification in Glo1-deficient mice [51]. However, the absence of alterations in the PFC AKR activity, and the small decrease in the HP (6%; Fig. 2d), albeit significant, is probably devoid of biological relevance. To test this possibility, other AKR substrates and expression analyses would be necessary. Alternatively, MGO degrading enzymes such as DJ1 and alcohol dehydrogenase are other routes to be investigated.

Brain MGO levels are increased within minutes after an i.p. injection [52] and remain elevated in the plasma for at least 4 h [21]; therefore, repeated MGO treatment would be expected to produce increased protein-MGO adducts. Immunohistochemical analysis of a major protein-MGO adduct, MG-H1, revealed a 30% increase in its levels in the HP at 25 mg/mg (Fig. 3d–f, h). A tendency to increased levels (1.7-fold increase) was also observed in the PFC at the same dose (Fig. 3a–c, g). However, no changes were observed in MG-H1 adducts in both brain structures at 50 mg/kg MGO (i.p.). It is puzzling that protein glycation remained unaltered at the higher MGO dose tested, despite it is somewhat in agreement with the absence of major changes in MGO detoxification (Fig. 2). In this regard, MGO adducts also remained unaltered in Glo1-KO mice [27, 51], suggesting an adaptive response would have been induced. Alternatively, specific protein target would be responsible for some effects of MGO, despite no overall changes in MG-H1 has been found (Fig. 3). The induction of alternative MGO-degrading systems needs to be verified before a grounded conclusion can be drawn.

Contrary to the in vitro response [11, 12, 36, 53, 54], no major changes were observed in the regulatory step in GSH synthesis, as GCL protein (Fig. 4a) and GSH levels (Fig. 4d), which remained at basal levels after MGO treatment. A similar pattern was observed regarding the activity of GR (Fig. 4b and e)

Fig. 2 Effects of MGO treatment on detoxification systems in the mice brain. Animals were treated for 7 days with MGO 25 mg/kg or 50 mg/kg, and 24 h later, tissues were collected. The relative protein levels of Glo1 (a) and Glo2 (b) and the activity of Glo1 (c) and AKR (d) were analyzed in the PFC and HP. Ponceau S was used as a protein loading control. Values are presented as scatter plot and mean + SEM ($n = 8-10$). Statistical differences are indicated as $*p < 0.05$, as compared to the saline-treated group (Ctl)



and TrxR (Fig. 4c and f), and despite GR protein presented a 42% increase, its activity remained at basal levels in animals treated with 50 mg/kg MGO. The same increase in GR protein

was observed in HT22 nerve cells treated with MGO, which was also paralleled by a decrease in GR activity [36]. In line with these results, it is possible that MGO treatment can lead to

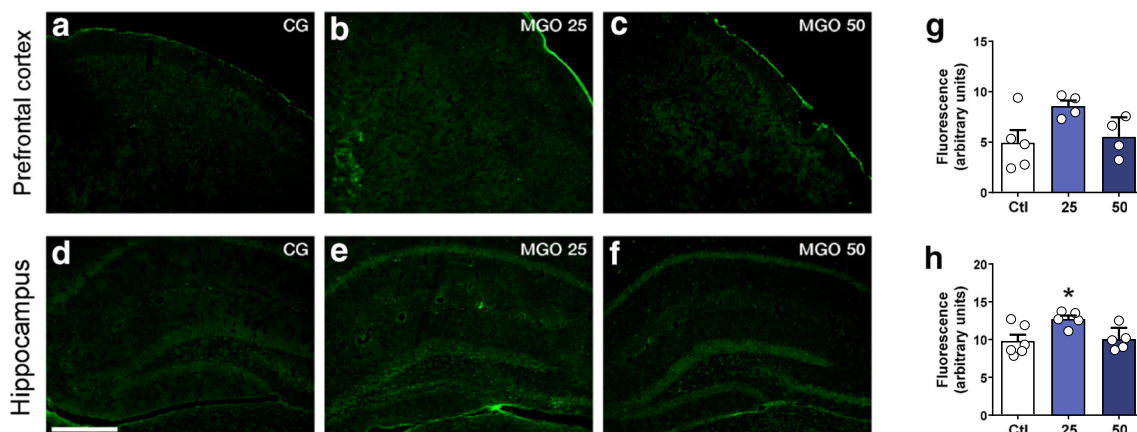


Fig. 3 Effects of MGO administration on MG-H1 adducts in the prefrontal cortex and hippocampus. Animals were treated for 7 days with MGO 25 mg/kg or 50 mg/kg, and 24 h later, tissues were collected. Representative images of MG-H1 adducts for PFC (a–c) and HP (d–f)

are presented along with their corresponding fluorescence quantification for PFC (g) and HP (h). Data are presented as scatter plot and mean + SEM ($n = 4-5$). Statistical differences are indicated as $*p < 0.05$, as compared to the saline-treated group (Ctl). Scale bar = 100 μm

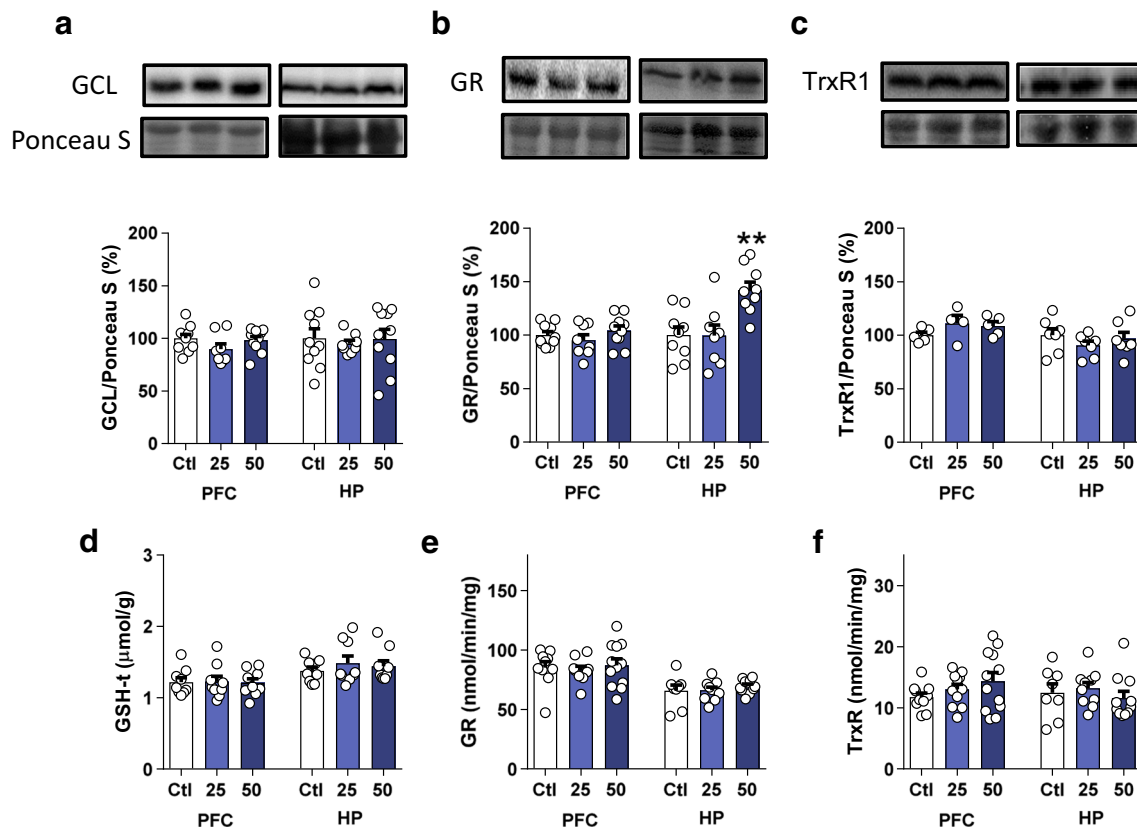


Fig. 4 Effects of repeated MGO administration on GSH and thioredoxin systems. Animals were treated for 7 days with MGO 25 mg/kg or 50 mg/kg, and 24 h later, tissues were collected. The relative protein levels of glutamate-cysteine ligase (GCL; **a**), glutathione reductase (GR; **b**), and thioredoxin reductase (TrxR; **c**). Total glutathione levels

(GSH-t, **d**) and the activity of GR (**e**) and TrxR (**f**) were analyzed in the PFC and HP. Ponceau S was used as a protein loading control. Values are presented as scatter plot and mean + SEM ($n = 8-12$). Statistical differences are indicated as $**p < 0.01$, as compared to the saline-treated group (Ctl)

inhibition by directly reacting with GR, as shown for TrxR [11]. Immunoprecipitation studies with GR would be necessary to clarify whether GR inhibition is due MGO adducts.

DARPP32 is an important signaling molecule, where phosphorylation at Thr34 leads to its activation, turning DARPP32 into a potent phosphatase 1 inhibitor [55]. Conversely, the opposite effect is observed when DARPP32 is phosphorylated at Thr75. Therefore, an increase in the Thr75/Thr34 ratio can be interpreted as a release of phosphatase 1 inhibition and by consequence dephosphorylating target proteins [55, 56]. DARPP32 protein levels were not altered ($p > 0.05$) by MGO treatment in the PFC (Fig. 5a) and HP (Fig. 5b); instead, MGO treatment promoted a decrease in the Thr34 phosphorylation, while it increased at site Thr75, resulting in a higher Thr75/Thr34 ratio (Fig. 5a). The Thr75/Thr34 ratio was not altered in the HP, and opposite to PFC, the phosphorylation site at Thr34 was increased, but at Thr75, it remained unaltered (Fig. 5b), indicating MGO preferentially affects the PFC. Interestingly, animals submitted to social defeat also presented increased Thr75 phosphorylation in the PFC, but not in the amygdala or hippocampus [57]. Overall, the data indicate an inhibition of DARPP32 signaling in the PFC, which would lead to increased dephosphorylating activity of protein

phosphatase 1. This response may be a consequence of the observed decrease in DA levels found in PFC (Fig. 7), which would result in a decreased DA signaling and increased Thr75/Thr34 ratio. Nevertheless, glutamate signaling would be involved in this response as well, since DARPP-32 participates in the translation of various states of glutamate input [58], which was not addressed in the present work. Given that MGO is considered a partial agonist of GABA_A receptors [52] and that GABAergic neurons can be dopaminergic [58], the interplay between DA depletion and activation of GABA_A receptors would also affect DARPP32 signaling.

The levels of tyrosine hydroxylase (TH), the rate-limiting step in DA synthesis [59], presented a slight increase (12%) in the PFC at 25 mg/kg MGO, which was not observed in the HP (Fig. 5c). The higher MGO dose (50 mg/kg) was unable to alter TH levels in both brain areas. A more aggressive treatment, such as intra-striatal administration of MGO, can decrease the number of tyrosine hydroxylase positive neurons and protein levels [60]. Conversely, dopaminergic cells (SH-SY5Y) presented increased tyrosine hydroxylase expression when treated with MGO [61]. At this point, it is unknown if MGO administered by an intraperitoneal route would result in the same responses.

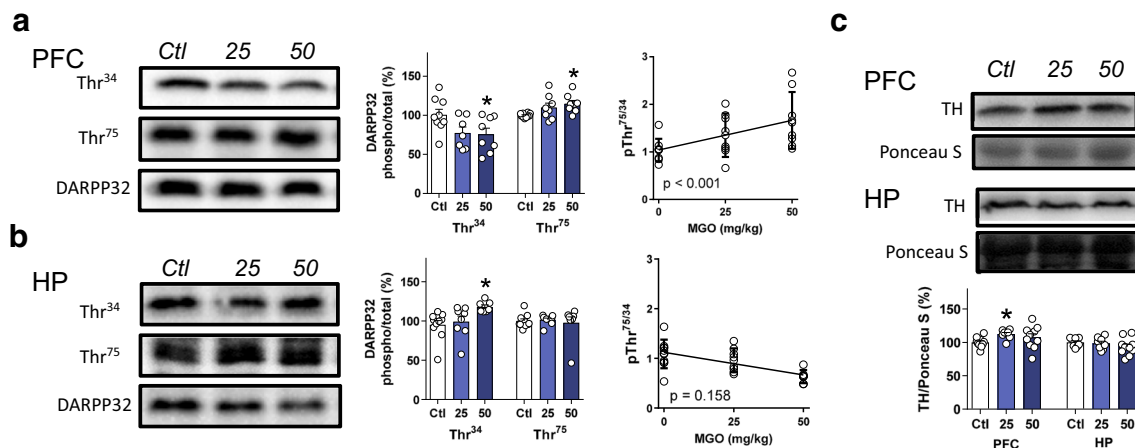


Fig. 5 Effects of MGO administration on DARPP32 phosphorylation, and the protein levels of tyrosine hydroxylase. Animals were treated for 7 days with MGO 25 mg/kg or 50 mg/kg, and 24 h later, tissues were collected and analyses were performed in the PFC and HP. Representative blot images of DARPP32 phosphorylation at sites Thr³⁴ and Thr⁷⁵ (**a** and **b**) are presented along with their respective quantifications (bar graphs). The band intensity of the DARPP32 phosphorylated forms was normalized to total DARPP32 protein content. In line graphs

(**a** and **b**), values are presented as scatter plot and mean \pm SD ($n = 8-10$). Correlation analysis showing the ratio between Thr⁷⁵/Thr³⁴ are also presented. Representative images of tyrosine hydroxylase (TH) blots are shown in **c**, along with their respective quantifications (bar graph). Ponceau S was used as a protein loading control for TH. The bar graph (**c**) presents scatter plot and mean + SEM ($n = 8-12$). Statistical differences are indicated as * $p < 0.05$, as compared to the saline-treated group (Ctl)

We have previously shown that MGO can induce an increase in the immobility time in the TST [21], in acute (15 min and 4 h) or repeated (6 days) treatments. These results are contrasting with previous publications showing that MGO treatment, or decreased Glo1 activity, can induce an antidepressant-like effect [29, 62]. Given the apparently contradictory results, and in order to exclude a possible bias due to genetic background, or a strain-related factor, we investigated two other mice strains. Therefore, we repeated the TST following MGO treatment and evaluated the immobility time in *Swiss* (Fig. 6a, d), C57BL/6 (Fig. 6b, e), and BALB/C (Fig. 6c, f) mice. Despite the small sample size ($n = 5-7$), a clear depression-like effect was induced by repeated MGO treatment for 8 days in all tested strains, ruling out an interference of genetic background. Murine models of depression, like the repeated defeat [31], and chronic unpredictable mild stress [30] have shown decreased Glo1 expression in HP and PFC, respectively, suggesting increased MGO levels may be associated to increased immobility in the TST. A previous study is in agreement with our results, as Glo1-KO mice present depression-like behavior [27]. The reasons for some studies have found antidepressant-like and other depression-like effects remain unknown and need to be considered. Our results showing the depression-like effect of MGO after repeated (7 days) MGO treatment are consistent, since the same depression-like effect was observed with different doses and treatment regimens [21], as well as in three mice strains (Fig. 6). It is worth of note that at the time of TST testing, blood MGO levels are at basal levels [21],

indicating the treatment effect may not be considered as a direct effect of MGO.

Disturbances in the homeostasis of monoamines are frequently associated with mood disorders and brain function [63]. As shown previously by our group, memory impairment and depression-like behavior were observed in mice treated with MGO. The same study showed that treatment with MGO for 11 days produced a $\sim 50\%$ decrease in the DA levels in the mice PFC. Here, we explored the possibility that BUP, a NE and DA reuptake inhibitor, would prevent DA depletion. MGO treatment for 11 days reproduced the previously observed depletion in DA in the PFC (Fig. 7a). Additionally, a 35% decrease in the levels of 5-HT (Fig. 7b) was also observed, but no changes were detected in the NE levels (Fig. 7c). The striatum presented preserved levels of DA (Fig. 7d), 5-HT (7E), and NE (Fig. 7f). The HP presented a tendency ($\sim 15\%$) for lower levels of 5-HT (Fig. 7g) and NE (Fig. 7h), but without statistical significance.

The underlying causes inducing depletion of neurotransmitters in MGO-treated mice remain to be established. An early report showed a free radical reaction of MGO and DA, 5-HT, and NE [64], which can potentially produce a number of toxic molecules. More recent evidences support this idea, as 5-HT and DA can produce highly toxic derivatives [65–68]. Another possible route for MGO toxicity relates to the activation of AGE receptor (RAGE) owing to long-lasting inflammation, which can also lead to the formation of toxic metabolites upstream and downstream of MGO production [69].

Co-administration of BUP and MGO produced an effect toward normalizing the levels of DA, 5-HT, and NE in the PFC, HP, and striatum, as values were not significantly

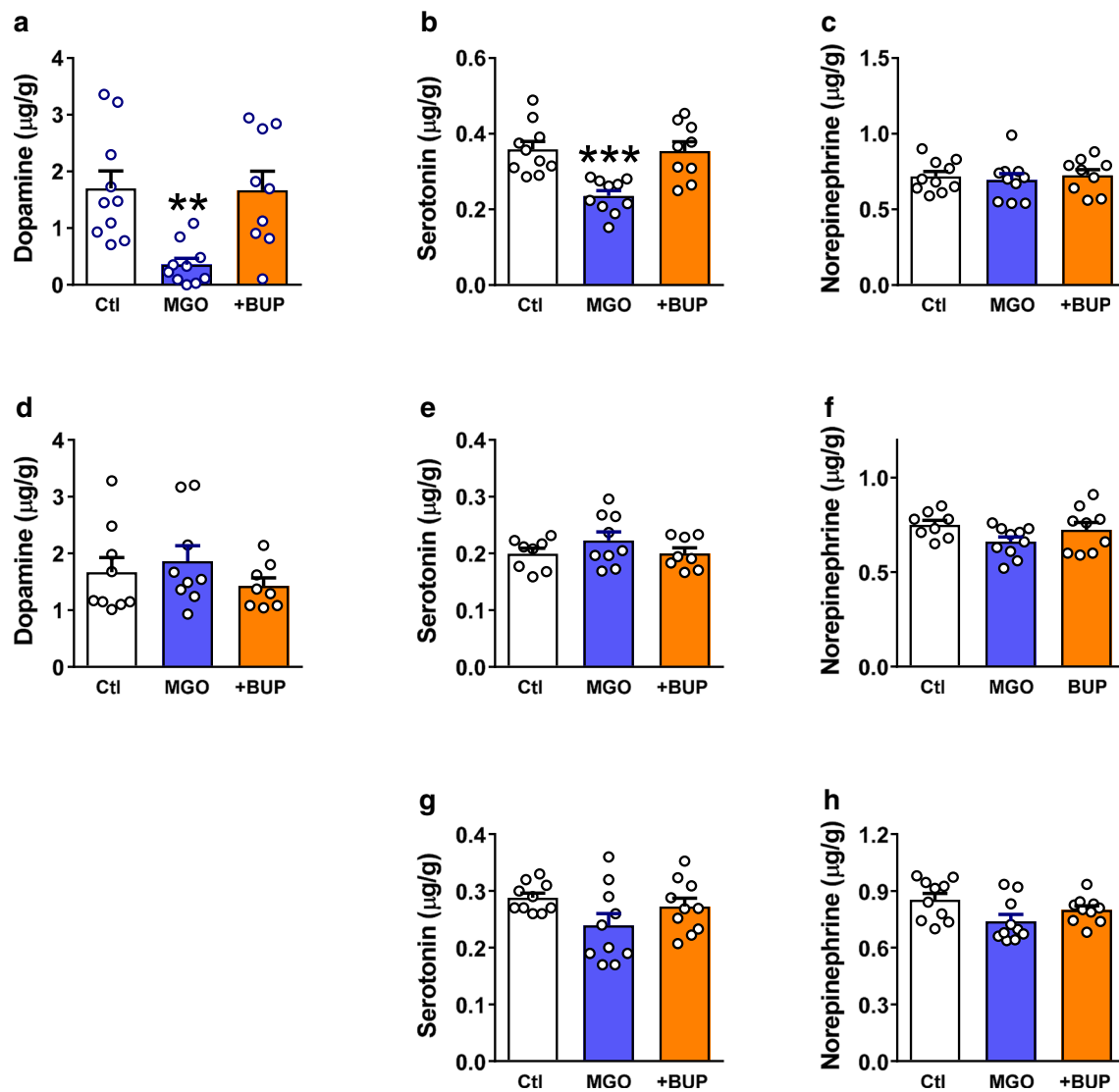


Fig. 7 Bupropion prevents dopamine and serotonin depletion in the PFC of MGO-treated mice. Swiss mice were treated for 12 days with saline (Ctl), MGO 50 mg/kg (MGO), or the combination BUP (10 mg/kg, p.o.) and MGO, as described in the “Materials and Methods” section. Twenty-four hours after the last MGO injection, tissues were collected for the measurements of dopamine (**a** and **d**), serotonin (**b**, **e**, and **g**), and

norepinephrine (**c**, **f**, and **h**) in the PFC (**a–c**), striatum (**d–f**), and HP (**g–h**) of mice. Dopamine was below the detection limit in the mice hippocampi. Values are presented as scatter plot and mean + SEM ($n = 8–10$). Statistical differences are indicated as $**p < 0.01$ and $***p < 0.001$, as compared to the saline-treated group (Ctl)

different, as compared to the control group. The results herein presented reinforce the known antidepressant action of BUP and indicate it would prevent the depressive-like behavior induced by MGO. Nevertheless, the exact mechanism responsible for such an effect in restoring the levels of DA and 5-HT in the PFC needs further investigation.

The present work confirms our previous data and strengthens the notion that MGO can induce a depression-like behavior through depleting monoamines. As shown in Fig. 8 a, the depression-like effect of MGO was abolished by a co-treatment with BUP. BUP per se did not alter the immobility time in the FST, neither did it affect spontaneous locomotion in the open field (Supplementary Fig. S2). The

fact that BUP also restored the levels of DA and 5-HT in the PFC suggests that MGO causes depression-like effect by depleting these neurotransmitters. However, further experiments are required to trace the origin of such disturbances by assessing the routes for synthesis and degradation of these neurotransmitters, as well as to verify the role of signaling pathways in such a response.

Several studies showed that MGO, or Glo1 expression, presents an association with anxiety and depression (trait or behavior). Some studies found that higher Glo1 levels are associated to anxiety and depression-like phenotypes [22, 29, 70]. Furthermore, inhibition or deletion of Glo1, or MGO treatment, can produce an antidepressant-like

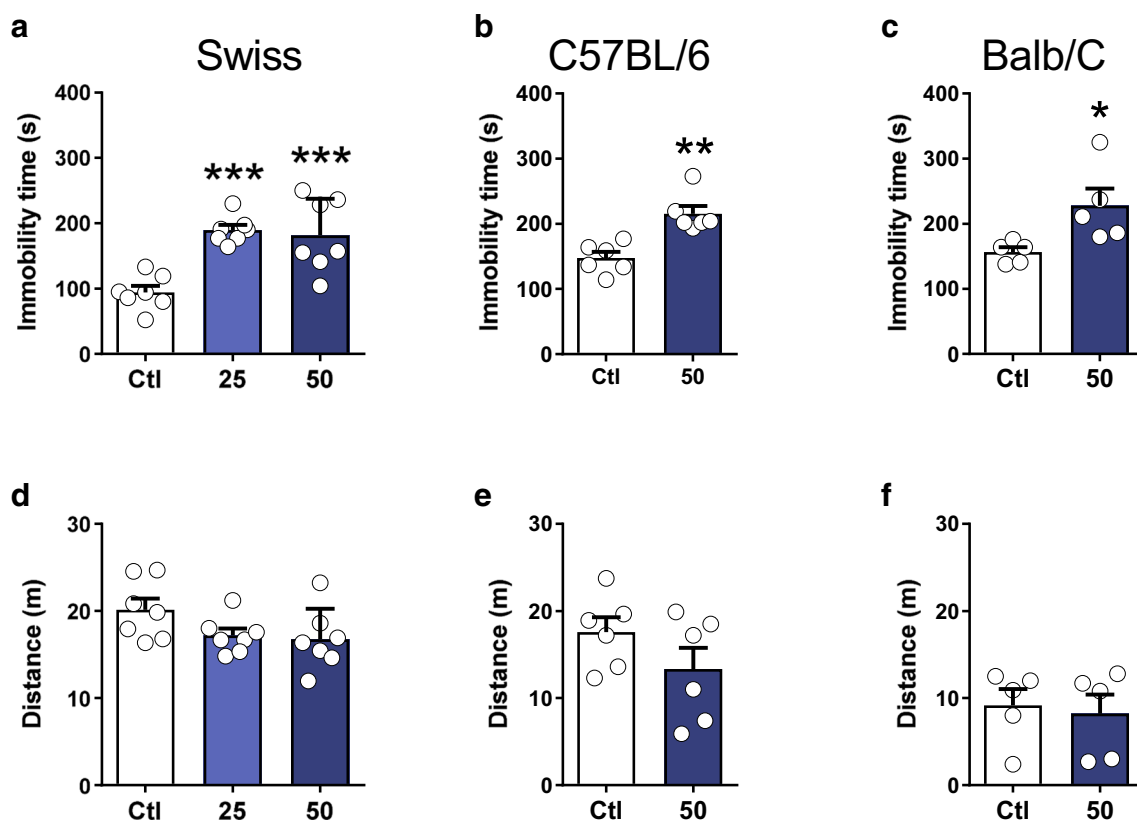


Fig. 6 Immobility time and locomotor activity in mice treated with MGO. Animals were treated for 7 days with MGO 25 mg/kg or 50 mg/kg and, 24 h later, submitted to the TST, followed by exposition to the open field. Immobility time in the TST (a–c) and ambulatory activity in the open field (d–f) were obtained for three mice strains:

Swiss (a and d), C57BL/6 (b and e), and BALB/C (c and f). Data are presented as scatter plot and mean + SEM ($n = 5-7$). Significant differences are indicated as $*p < 0.05$, $**p < 0.01$, and $***p < 0.001$, as compared to the saline-treated control group (Ctl)

phenotype [26, 71–73]. The higher doses employed in the current work contrasts to the observed beneficial effects of MGO at lower doses and more prolonged treatment. MGO (5 mM/kg per day) can produce antidepressant-like effect, which was linked to induction of neurotrophic factors, such as BDNF, and was also associated to neurogenesis [72]. As opposing to these results, MGO treatment decreased the sucrose preference, indicating MGO can induce a depression-like behavior [74]. Moreover, lower levels of *Glo1* mRNA in peripheral cells correlated with major depressive disorder [28]. Subjects with this pathology presented higher *Glo1* levels [75], and *Glo1*-KO mice showed depressive-like behavior [27]. Although the literature expresses contradictory data, these last mentioned evidences are corroborating our data (Figs. 6 and 8), showing that MGO can induce depression-like behavior after repeated treatment, as well as acute treatment (15 min and 4 h) [21].

The working memory deficits previously found in MGO-treated mice [21] were prevented by BUP + MGO treatment (Fig. 8b); however, long-term spatial memory was not (Fig. 8c). Swiss mice treated with MGO showed significantly decreased alternation rate, when compared with the control group, indicating working memory deficit, which was

prevented by BUP co-treatment (Fig. 8b). Locomotor activity of mice in the Y maze was not altered by the treatments, as no statistical difference was found in the total number of arm entries among the groups, thus indicating no biases due to altered locomotor activity (Fig. 8e).

BUP treatment was also associated with a better performance of mental processing speed in humans, which is very dependent on the PFC and working memory [76]. DA signaling in the PFC appears to play a critical role in animals' performance in both working memory and selective attention tasks [77]. Therefore, the protective effect of BUP in preventing DA depletion suggests that normalization on working memory was involved with DA replenishment, which remains to be confirmed, and other potential mechanisms need to be considered. Given that BUP induces a transient increase in the brain levels of DA and NE [78, 79], it is not expected that this effect remains active for 24 h after injection. Therefore, the behavioral changes observed can be understood as long-term effects of BUP, in which DA and 5-HT are believed to remain at basal levels, but unfortunately, we do not have data to support this hypothesis.

In the OLT, the control group explored the relocated object B for more than 50% of the total exploratory time, thereby

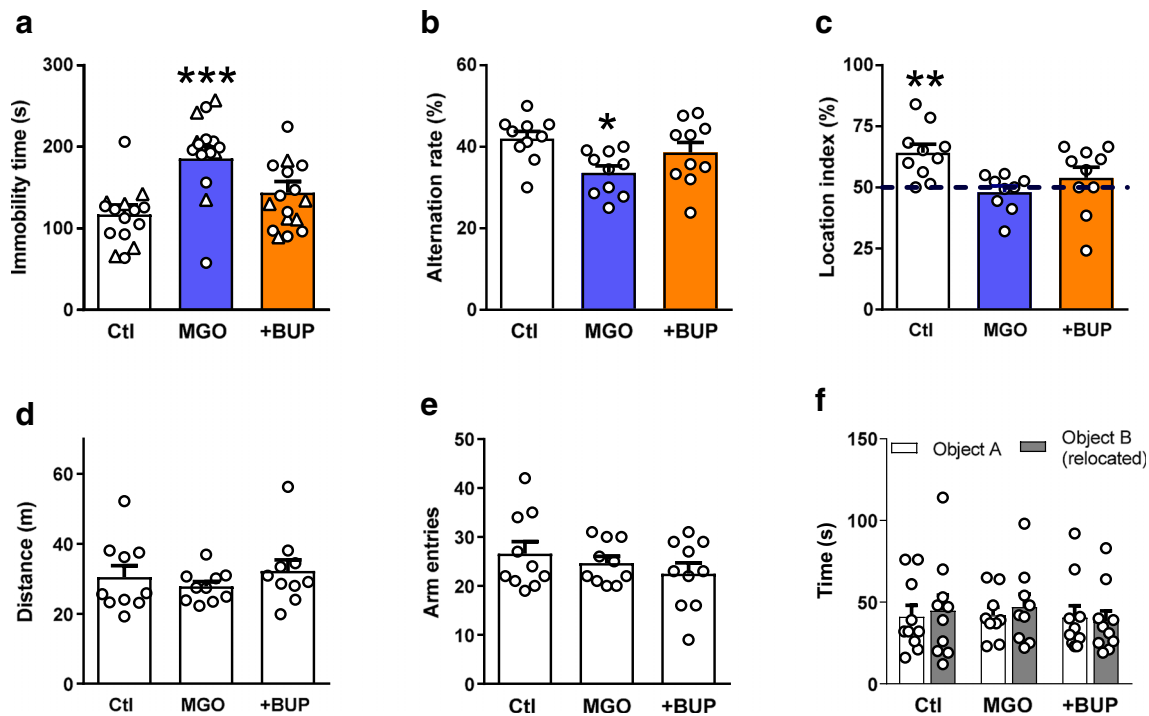


Fig. 8 Bupropion prevented the increase in the immobility time and working memory deficit of mice treated with MGO. Swiss mice were treated for 11 days with saline (Ctl), MGO 50 mg/kg (MGO), or the combination of MGO and bupropion 10 mg/kg, p.o. (+BUP), as described in the “Materials and Methods” section. Twenty-four hours after the seventh MGO injection, the immobility time was assessed by the TST (a) and the ambulatory activity in the open field (d). The spontaneous alternation rate was measured in the Y-maze test (b) 24 h after the sixth MGO injection, as well as the corresponding ambulatory activity (e). The long-term spatial memory of Swiss mice was assessed in the test session

showing memory retention (Fig. 8c). Mice treated with MGO or BUP + MGO did not present differences in the object location index, when compared to 50%, indicating memory impairment (Fig. 8c). In the training session, no statistical differences were found between the exploratory time periods of the two identical objects (Fig. 8f). Therefore, results showed that BUP was unable to prevent the long-term spatial memory impairment induced by MGO.

Since DA is the main neurotransmitter involved in the mesolimbic reward pathways, it has been proposed that an increase in dopaminergic neurotransmission might counteract the prominent symptom of depression anhedonia, as well as modulating learning and memory [80]. Nevertheless, the role for 5-HT has to be considered, as MGO also depleted 5-HT in the PFC. BUP produced antimnemonic effect in mice exposed to scopolamine [33]. In our study, BUP abrogated the MGO-induced cortical DA and 5-HT depletion, as well as the depression-like behavior and working memory impairment, but failed to restore long-term spatial memory.

Despite IHC results failed to detect alteration in MG-H1 at the highest dose tested, AGEs/RAGE signaling are known to be involved in a variety of neuropathies and in cognitive

dysfunction [81, 82]. In agreement to this idea, a work of our group [83] showed that FPS-ZM1, a selective RAGE antagonist that is permeable to the blood-brain barrier, restored short-term aversive and working memory, but failed to restore short-term or long-term spatial memory impairment, induced by repeated MGO treatment [83]. These results indicate that some effects of MGO can possibly be attributed to RAGE activation, as its inhibitor prevented some effects but failed to prevent others. A similar scenario was observed as shown in Fig. 8, since BUP failed to restore the long-term spatial memory. Nevertheless, BUP was effective in decreasing the immobility time in the FST and in normalizing the alternation rate in the Y-maze. It is conceivable to think that multiple action mechanisms would be responsible for the observed results, suggesting memory deficits induced by MGO depend, at least in part, on mechanisms other than DA and 5-HT depletion.

dysfunction [81, 82]. In agreement to this idea, a work of our group [83] showed that FPS-ZM1, a selective RAGE antagonist that is permeable to the blood-brain barrier, restored short-term aversive and working memory, but failed to restore short-term or long-term spatial memory impairment, induced by repeated MGO treatment [83]. These results indicate that some effects of MGO can possibly be attributed to RAGE activation, as its inhibitor prevented some effects but failed to prevent others. A similar scenario was observed as shown in Fig. 8, since BUP failed to restore the long-term spatial memory. Nevertheless, BUP was effective in decreasing the immobility time in the FST and in normalizing the alternation rate in the Y-maze. It is conceivable to think that multiple action mechanisms would be responsible for the observed results, suggesting memory deficits induced by MGO depend, at least in part, on mechanisms other than DA and 5-HT depletion.

Concluding Remarks

We found little evidence that Glo1/Glo2, Trx/TrxR, and GSH/GCL/GR systems are affected by repeated MGO treatment for

7 days. We showed higher DARPP32 Thr⁷⁵/Thr³⁴ phosphorylation ratio in the PFC, but not in the HP, of MGO-treated mice, a signaling route depending on glutamate and DA, that needs further investigation. The present study confirmed that repeated treatment with MGO produced a depression-like phenotype, which was reproduced in three different mice strains. DA and 5-HT depletion was observed in the PFC; however, the mechanisms responsible for this decrease remain to be established. Some possibilities include formation of toxic products from MGO reaction with other molecules, such as DA and 5-HT, or by interfering with their synthesis, degradation, and transport. Repeated MGO treatment was also able to impair working and long-term memory. The atypical antidepressant BUP not only prevented DA and 5-HT depletion but also suppressed the depression-like phenotype and restored working memory. Interestingly, in a parallel study, aversive and working memory deficits induced by MGO were prevented by a RAGE antagonist [83], indicating that action mechanisms other than DA and 5-HT depletion also need to be taken in account when the effects of MGO are considered.

Acknowledgments GRLA, JCS, and AES received graduation scholarships awarded by the Coordination of Improvement of Higher Education Personnel (CAPES, Brazil). IS and BS received undergraduate scholarships awarded by the Brazilian National Development and Research Council (CNPq). ALD, RBL, and AFDB are recipients of research productivity fellowships from CNPq. The excellent technical assistance of Gabriela Karasiak is deeply acknowledged. This work was supported by CNPq (#462333/2014-0; #306204/2014-2; #307057/2018-1).

Authors' Contributions GRLA, JCS, and ALD contributed to the experimental design, data analysis, and writing of the manuscript. GRLA, JCS, MPC, and IS performed the behavioral experiments. GRLA and IS performed the HPLC analysis. GRLA, IS, and BS performed the biochemical analyses and Western blots. GRLA, ISH, and RBL performed the DARPP32 experiment. GCP, AFDB, and GRLA performed the IHC analysis. All authors gave input to the manuscript. All authors read and approved the final manuscript.

Compliance with Ethical Standards

Conflict of Interest The authors that they have declare no conflict of interest.

Ethical Approval The animal ethics committee of the Federal University of Santa Catarina (CEUA-UFSC, #7245210616) approved the experiments. All efforts were made to reduce the number of mice used and animal suffering, which is in conformity with the *Guide for the Care and Use of Laboratory Animals*, National Institutes of Health.

Consent for Publication Not applicable.

References

- Thornalley PJ, Rabbani N (2011) Glyoxalase in tumorigenesis and multidrug resistance. *Semin Cell Dev Biol* 22:318–325. <https://doi.org/10.1016/j.semcdb.2011.02.006>
- Rabbani N, Xue M, Thornalley PJ (2016) Dicarboxyls and glyoxalase in disease mechanisms and clinical therapeutics. *Glycoconj J* 33:513–525. <https://doi.org/10.1007/s10719-016-9705-z>
- Beeri MS, Moshier E, Schmeidler J, Godbold J, Uribarri J, Reddy S, Sano M, Grossman HT et al (2011) Serum concentration of an inflammatory glycotoxin, methylglyoxal, is associated with increased cognitive decline in elderly individuals. *Mech Ageing Dev* 132:583–587. <https://doi.org/10.1016/j.mad.2011.10.007>
- Kuhla B, Lüth H-J, Haferburg D et al (2005) Methylglyoxal, glyoxal, and their detoxification in Alzheimer's disease. *Ann N Y Acad Sci* 1043:211–216. <https://doi.org/10.1196/annals.1333.026>
- Allaman I, Bélanger M, Magistretti PJ (2015) Methylglyoxal, the dark side of glycolysis. *Front Neurosci* 9:23. <https://doi.org/10.3389/fnins.2015.00023>
- Mindnich RD, Penning TM (2009) Aldo-keto reductase (AKR) superfamily: genomics and annotation. *Hum Genomics* 3:362–370
- Richarme G, Mihoub M, Dairou J, Bui LC, Leger T, Lamouri A (2015) Parkinsonism-associated protein DJ-1/Park7 is a major protein deglycase that repairs methylglyoxal- and glyoxal-glycated cysteine, arginine, and lysine residues. *J Biol Chem* 290:1885–1897. <https://doi.org/10.1074/jbc.M114.597815>
- Richarme G, Abdallah J, Mathas N, Gautier V, Dairou J (2018) Further characterization of the Maillard deglycase DJ-1 and its prokaryotic homologs, deglycase 1/Hsp31, deglycase 2/YhbO, and deglycase 3/YajL. *Biochem Biophys Res Commun* 503:703–709. <https://doi.org/10.1016/j.bbrc.2018.06.064>
- Mihoub M, Abdallah J, Richarme G (2017) Protein repair from glycation by glyoxals by the DJ-1 family Maillard deglycases. In: Ariga H, Iguchi-Arigo SMM (eds) DJ-1/PARK7 protein: Parkinson's disease, cancer and oxidative stress-induced diseases. Springer, Singapore, pp. 133–147
- Thornalley PJ (2003) Glyoxalase I—structure, function and a critical role in the enzymatic defence against glycation. *Biochem Soc Trans* 31:1343–1348. <https://doi.org/10.1042/bst0311343>
- Dafre AL, Goldberg J, Wang T, Spiegel DA, Maher P (2015) Methylglyoxal, the foe and friend of glyoxalase and Trx/TrxR systems in HT22 nerve cells. *Free Radic Biol Med* 89:8–19. <https://doi.org/10.1016/j.freeradbiomed.2015.07.005>
- Dafre AL, Schmitz AE, Maher P (2017) Methylglyoxal-induced AMPK activation leads to autophagic degradation of thioredoxin 1 and glyoxalase 2 in HT22 nerve cells. *Free Radic Biol Med* 108:270–279. <https://doi.org/10.1016/j.freeradbiomed.2017.03.028>
- Rabbani N, Xue M, Thornalley PJ (2016) Methylglyoxal-induced dicarbonyl stress in aging and disease: first steps towards glyoxalase 1-based treatments. *Clin Sci Lond Engl* 130:1677–1696. <https://doi.org/10.1042/CS20160025>
- Burnside SW, Hardingham GE (2017) Transcriptional regulators of redox balance and other homeostatic processes with the potential to alter neurodegenerative disease trajectory. *Biochem Soc Trans* 45:1295–1303. <https://doi.org/10.1042/BST20170013>
- Carlberg I, Mannervik B (1985) Glutathione reductase. *Methods Enzymol* 113:484–490
- Holmgren A, Björnstedt M (1995) Thioredoxin and thioredoxin reductase. *Methods Enzymol* 252:199–208. [https://doi.org/10.1016/0076-6879\(95\)52023-6](https://doi.org/10.1016/0076-6879(95)52023-6)
- Huang X, Wang F, Chen W, Chen Y, Wang N, von Maltzan K (2012) Possible link between the cognitive dysfunction associated with diabetes mellitus and the neurotoxicity of methylglyoxal. *Brain Res* 1469:82–91. <https://doi.org/10.1016/j.brainres.2012.06.011>
- Kong X, Ma M, Huang K, Qin L, Zhang HM, Yang Z, Li XY, Su Q (2014) Increased plasma levels of the methylglyoxal in patients with newly diagnosed type 2 diabetes 2. *J Diabetes* 6:535–540. <https://doi.org/10.1111/1753-0407.12160>

19. Srikanth V, Westcott B, Forbes J, Phan TG, Beare R, Venn A, Pearson S, Greenaway T et al (2013) Methylglyoxal, cognitive function and cerebral atrophy in older people. *J Gerontol A Biol Sci Med Sci* 68:68–73. <https://doi.org/10.1093/gerona/gls100>
20. Watanabe K, Okada K, Fukabori R, Hayashi Y, Asahi K, Terawaki H, Kobayashi K, Watanabe T et al (2014) Methylglyoxal (MG) and cerebro-renal interaction: does long-term orally administered MG cause cognitive impairment in normal Sprague-Dawley rats? *Toxins* 6:254–269. <https://doi.org/10.3390/toxins6010254>
21. Szczepaniak JC, de Almeida GRL, Cunha MP, Dafre AL (2020) Repeated methylglyoxal treatment depletes dopamine in the prefrontal cortex, and causes memory impairment and depressive-like behavior in mice. *Neurochem Res* 45:354–370. <https://doi.org/10.1007/s11064-019-02921-2>
22. Krömer SA, Kessler MS, Milfay D, Birg IN, Bunck M, Czibere L, Panhuysen M, Pütz B et al (2005) Identification of glyoxalase-I as a protein marker in a mouse model of extremes in trait anxiety. *J Neurosci* 25:4375–4384. <https://doi.org/10.1523/JNEUROSCI.0115-05.2005>
23. Hovatta I, Tennant RS, Helton R, Marr RA, Singer O, Redwine JM, Ellison JA, Schadt EE et al (2005) Glyoxalase 1 and glutathione reductase 1 regulate anxiety in mice. *Nature* 438:662–666. <https://doi.org/10.1038/nature04250>
24. Thornalley PJ (2006) Unease on the role of glyoxalase 1 in high-anxiety-related behaviour. *Trends Mol Med* 12:195–199. <https://doi.org/10.1016/j.molmed.2006.03.004>
25. Williams R, Lim JE, Harr B, Wing C, Walters R, Distler MG, Teschke M, Wu C et al (2009) A common and unstable copy number variant is associated with differences in Glo1 expression and anxiety-like behavior. *PLoS One* 4:e4649. <https://doi.org/10.1371/journal.pone.0004649>
26. Distler MG, Palmer AA (2012) Role of glyoxalase 1 (Glo1) and methylglyoxal (MG) in behavior: recent advances and mechanistic insights. *Front Genet* 3:250. <https://doi.org/10.3389/fgene.2012.00250>
27. Jang S, Kwon DM, Kwon K, Park C (2017) Generation and characterization of mouse knockout for glyoxalase 1. *Biochem Biophys Res Commun* 490:460–465. <https://doi.org/10.1016/j.bbrc.2017.06.063>
28. Fujimoto M, Uchida S, Watanuki T, Wakabayashi Y, Otsuki K, Matsubara T, Suetsugi M, Funato H et al (2008) Reduced expression of glyoxalase-1 mRNA in mood disorder patients. *Neurosci Lett* 438:196–199. <https://doi.org/10.1016/j.neulet.2008.04.024>
29. Benton CS, Miller BH, Skwerer S, Suzuki O, Schultz LE, Cameron MD, Marron JS, Pletcher MT et al (2012) Evaluating genetic markers and neurobiochemical analytes for fluoxetine response using a panel of mouse inbred strains. *Psychopharmacology* 221:297–315. <https://doi.org/10.1007/s00213-011-2574-z>
30. Yang Y, Yang D, Tang G, Zhou C, Cheng K, Zhou J, Wu B, Peng Y et al (2013) Proteomics reveals energy and glutathione metabolic dysregulation in the prefrontal cortex of a rat model of depression. *Neuroscience* 247:191–200. <https://doi.org/10.1016/j.neuroscience.2013.05.031>
31. Patki G, Solanki N, Atrooz F, Allam F, Salim S (2013) Depression, anxiety-like behavior and memory impairment are associated with increased oxidative stress and inflammation in a rat model of social stress. *Brain Res* 1539:73–86. <https://doi.org/10.1016/j.brainres.2013.09.033>
32. Deang KT, Sidi H, Zakaria H, Adam RL, Das S, Hatta NH, Hatta MH, Wee KW (2019) The novelty of bupropion as a dopaminergic antidepressant for the treatment of adult attention deficit hyperactive disorder. *Curr Drug Targets* 20:210–219. <https://doi.org/10.2174/1389450118666170511145628>
33. Cunha MP, Machado DG, Bettio LEB, Capra JC, Rodrigues ALS (2008) Interaction of zinc with antidepressants in the tail suspension test. *Prog Neuro-Psychopharmacol Biol Psychiatry* 32:1913–1920. <https://doi.org/10.1016/j.pnpbp.2008.09.006>
34. Nadar JS, Kale PP, Kadu PK, Prabhavalkar K, Dhangar R (2018) Potentiation of antidepressant effects of agomelatine and bupropion by hesperidin in mice. *Neurol Res Int* 2018:1–7. <https://doi.org/10.1155/2018/9828639>
35. Kruk-Słomka M, Michalak A, Budzyńska B, Biała G (2014) A comparison of mecamlamine and bupropion effects on memory-related responses induced by nicotine and scopolamine in the novel object recognition test in mice. *Pharmacol Rep* 66:638–646. <https://doi.org/10.1016/j.pharep.2014.02.002>
36. Schmitz AE, de Souza LF, Dos Santos B et al (2017) Methylglyoxal-induced protection response and toxicity: role of glutathione reductase and thioredoxin systems. *Neurotox Res* 32:340–350. <https://doi.org/10.1007/s12640-017-9738-5>
37. Wong M-L, Licinio J (2001) Research and treatment approaches to depression. *Nat Rev Neurosci* 2:343–351. <https://doi.org/10.1038/35072566>
38. Tietze F (1969) Enzymic method for quantitative determination of nanogram amounts of total and oxidized glutathione: applications to mammalian blood and other tissues. *Anal Biochem* 27:502–522. [https://doi.org/10.1016/0003-2697\(69\)90064-5](https://doi.org/10.1016/0003-2697(69)90064-5)
39. Arai M, Nihonmatsu-Kikuchi N, Itokawa M, Rabbani N, Thornalley PJ (2014) Measurement of glyoxalase activities. *Biochem Soc Trans* 42:491–494. <https://doi.org/10.1042/BST20140010>
40. Srivastava S, Watowich SJ, Petrash JM, Srivastava SK, Bhatnagar A (1999) Structural and kinetic determinants of aldehyde reduction by aldose reductase. *Biochemistry* 38:42–54. <https://doi.org/10.1021/bi981794l>
41. Bradford MM (1976) A rapid and sensitive method for the quantitation of microgram quantities of protein utilizing the principle of protein-dye binding. *Anal Biochem* 72:248–254. [https://doi.org/10.1016/0003-2697\(76\)90527-3](https://doi.org/10.1016/0003-2697(76)90527-3)
42. De Benedetto GE, Fico D, Pennetta A et al (2014) A rapid and simple method for the determination of 3,4-dihydroxyphenylacetic acid, norepinephrine, dopamine, and serotonin in mouse brain homogenate by HPLC with fluorimetric detection. *J Pharm Biomed Anal* 98:266–270. <https://doi.org/10.1016/j.jpba.2014.05.039>
43. Steru L, Chermat R, Thierry B, Simon P (1985) The tail suspension test: a new method for screening antidepressants in mice. *Psychopharmacology* 85:367–370. <https://doi.org/10.1007/bf00428203>
44. Belzung C (1999) Measuring rodent exploratory behavior. In: Crusio WE, Gerlai RT (eds) *Techniques in the behavioral and neural sciences*. Elsevier, pp. 738–749
45. Prut L, Belzung C (2003) The open field as a paradigm to measure the effects of drugs on anxiety-like behaviors: a review. *Eur J Pharmacol* 463:3–33. [https://doi.org/10.1016/s0014-2999\(03\)01272-x](https://doi.org/10.1016/s0014-2999(03)01272-x)
46. Tolman EC (1925) Purpose and cognition: the determiners of animal learning. *Psychol Rev* 32:285–297. <https://doi.org/10.1037/h0072784>
47. Dember WN, Fowler H (1958) Spontaneous alternation behavior. *Psychol Bull* 55:412–428. <https://doi.org/10.1037/h0045446>
48. Assini FL, Duzzioni M, Takahashi RN (2009) Object location memory in mice: pharmacological validation and further evidence of hippocampal CA1 participation. *Behav Brain Res* 204:206–211. <https://doi.org/10.1016/j.bbr.2009.06.005>
49. Vogel-Ciernia A, Wood MA (2014) Examining object location and object recognition memory in mice. *Curr Protoc Neurosci* 69:8.31.1–8.31.17. <https://doi.org/10.1002/0471142301.ns0831s69>
50. Shin MJ, Kim DW, Lee YP, Ahn EH, Jo HS, Kim DS, Kwon OS, Kang TC et al (2014) Tat-glyoxalase protein inhibits against ischemic neuronal cell damage and ameliorates ischemic injury. *Free*

- Radic Biol Med 67:195–210. <https://doi.org/10.1016/j.freeradbiomed.2013.10.815>
51. Schumacher D, Morgenstern J, Oguchi Y, Volk N, Kopf S, Groener JB, Nawroth PP, Fleming T et al (2018) Compensatory mechanisms for methylglyoxal detoxification in experimental & clinical diabetes. *Mol Metab* 18:143–152. <https://doi.org/10.1016/j.molmet.2018.09.005>
 52. Distler MG, Plant LD, Sokoloff G, Hawk AJ, Aneas I, Wuenschell GE, Termini J, Meredith SC et al (2012) Glyoxalase 1 increases anxiety by reducing GABAA receptor agonist methylglyoxal. *J Clin Invest* 122:2306–2315. <https://doi.org/10.1172/JCI61319>
 53. Hansen F, Pandolfo P, Galland F, Torres FV, Dutra MF, Batassini C, Guerra MC, Leite MC et al (2016) Methylglyoxal can mediate behavioral and neurochemical alterations in rat brain. *Physiol Behav* 164:93–101. <https://doi.org/10.1016/j.physbeh.2016.05.046>
 54. Hansen F, Galland F, Lirio F, de Souza DF, da Ré C, Pacheco RF, Vizuete AF, Quincozes-Santos A et al (2017) Methylglyoxal induces changes in the glyoxalase system and impairs glutamate uptake activity in primary astrocytes. *Oxidative Med Cell Longev* 2017:9574201–9574211. <https://doi.org/10.1155/2017/9574201>
 55. Svenningsson P, Nishi A, Fisone G, Girault JA, Nairn AC, Greengard P (2004) DARPP-32: an integrator of neurotransmission. *Annu Rev Pharmacol Toxicol* 44:269–296. <https://doi.org/10.1146/annurev.pharmtox.44.101802.121415>
 56. Bibb JA, Snyder GL, Nishi A, Yan Z, Meijer L, Fienberg AA, Tsai LH, Kwon YT et al (1999) Phosphorylation of DARPP-32 by Cdk5 modulates dopamine signalling in neurons. *Nature* 402:669–671. <https://doi.org/10.1038/45251>
 57. Jin H-M, Shrestha Muna S, Bagalkot TR, Cui Y, Yadav BK, Chung YC (2015) The effects of social defeat on behavior and dopaminergic markers in mice. *Neuroscience* 288:167–177. <https://doi.org/10.1016/j.neuroscience.2014.12.043>
 58. Yger M, Girault J-A (2011) DARPP-32, Jack of all trades... master of which? *Front Behav Neurosci* 5. <https://doi.org/10.3389/fnbeh.2011.00056>
 59. Juárez Olguín H, Calderón Guzmán D, Hernández García E, Barragán Mejía G (2016) The role of dopamine and its dysfunction as a consequence of oxidative stress. *Oxidative Med Cell Longev* 2016:9730467–9730413. <https://doi.org/10.1155/2016/9730467>
 60. Sharma N, Rao SP, Kalivendi SV (2019) The deglycase activity of DJ-1 mitigates α -synuclein glycation and aggregation in dopaminergic cells: Role of oxidative stress mediated downregulation of DJ-1 in Parkinson's disease. *Free Radic Biol Med* 135:28–37. <https://doi.org/10.1016/j.freeradbiomed.2019.02.014>
 61. Xie B, Lin F, Peng L, Ullah K, Wu H, Qing H, Deng Y (2014) Methylglyoxal increases dopamine level and leads to oxidative stress in SH-SY5Y cells. *Acta Biochim Biophys Sin* 46:950–956. <https://doi.org/10.1093/abbs/gmu094>
 62. Hamsch B, Chen B-G, Brenndörfer J, Meyer M, Avrabos C, Maccarrone G, Liu RH, Eder M et al (2010) Methylglyoxal-mediated axiolysis involves increased protein modification and elevated expression of glyoxalase 1 in the brain. *J Neurochem* 113:1240–1251. <https://doi.org/10.1111/j.1471-4159.2010.06693.x>
 63. Boku S, Nakagawa S, Toda H, Hishimoto A (2018) Neural basis of major depressive disorder: beyond monoamine hypothesis. *Psychiatry Clin Neurosci* 72:3–12. <https://doi.org/10.1111/pcn.12604>
 64. Szent-Györgyi A, McLaughlin JA (1975) Interaction of glyoxal and methylglyoxal with biogenic amines. *Proc Natl Acad Sci U S A* 72:1610–1611. <https://doi.org/10.1073/pnas.72.4.1610>
 65. Xie B, Lin F, Ullah K, Peng L, Ding W, Dai R, Qing H, Deng Y (2015) A newly discovered neurotoxin ADTIQ associated with hyperglycemia and Parkinson's disease. *Biochem Biophys Res Commun* 459:361–366. <https://doi.org/10.1016/j.bbrc.2015.02.069>
 66. Sachin LS, Chary RN, Pavankumar P, Prabhakar S (2018) Identification and characterization of reaction products of 5-hydroxytryptamine with methylglyoxal and glyoxal by liquid chromatography/tandem mass spectrometry. *Rapid Commun Mass Spectrom* 32:1529–1539. <https://doi.org/10.1002/rcm.8195>
 67. Goldstein DS (2020) The catecholaldehyde hypothesis: where MAO fits in. *J Neural Transm* 127:169–177. <https://doi.org/10.1007/s00702-019-02106-9>
 68. Tang Y, Hu C, Sang S (2020) Characterization of reaction products and mechanisms between serotonin and methylglyoxal in model reactions and mice. *J Agric Food Chem* 68:2437–2444. <https://doi.org/10.1021/acs.jafc.0c00071>
 69. Agostini A, Yuchun D, Li B, Kendall DA, Pardon MC (2020) Sex-specific hippocampal metabolic signatures at the onset of systemic inflammation with lipopolysaccharide in the APP^{swe}/PS1^{dE9} mouse model of Alzheimer's disease. *Brain Behav Immun* 83:87–111. <https://doi.org/10.1016/j.bbi.2019.09.019>
 70. Ditzen C, Jastorff AM, Kessler MS, Bunck M, Teplytska L, Erhardt A, Krömer SA, Varadarajulu J et al (2006) Protein biomarkers in a mouse model of extremes in trait anxiety. *Mol Cell Proteomics* 5:1914–1920. <https://doi.org/10.1074/mcp.M600088-MCP200>
 71. McMurray KMJ, Ramaker MJ, Barkley-Levenson AM et al (2018) Identification of a novel, fast-acting GABAergic antidepressant. *Mol Psychiatry* 23:384–391. <https://doi.org/10.1038/mp.2017.14>
 72. Wu Z, Fu Y, Yang Y, et al (2018) Gating TrkB switch by methylglyoxal enables GLO1 as a target for depression. *bioRxiv* 435867. <https://doi.org/10.1101/435867>
 73. Perez C, Barkley-Levenson AM, Dick BL, Glatt PF, Martinez Y, Siegel D, Momper JD, Palmer AA et al (2019) Metal-binding pharmacophore library yields the discovery of a glyoxalase 1 inhibitor. *J Med Chem* 62:1609–1625. <https://doi.org/10.1021/acs.jmedchem.8b01868>
 74. Zhang S, Jiao T, Chen Y, Gao N, Zhang L, Jiang M (2014) Methylglyoxal induces systemic symptoms of irritable bowel syndrome. *PLoS One* 9:e105307. <https://doi.org/10.1371/journal.pone.0105307>
 75. Tanna VL, Wilson AF, Winokur G, Elston RC (1989) Linkage analysis of pure depressive disease. *J Psychiatr Res* 23:99–107. [https://doi.org/10.1016/0022-3956\(89\)90001-0](https://doi.org/10.1016/0022-3956(89)90001-0)
 76. Lara AH, Wallis JD (2015) The role of prefrontal cortex in working memory: a mini review. *Front Syst Neurosci* 9. <https://doi.org/10.3389/fnysys.2015.00173>
 77. Goldman-Rakic PS, Muly EC, Williams GV (2000) D(1) receptors in prefrontal cells and circuits. *Brain Res Brain Res Rev* 31:295–301. [https://doi.org/10.1016/s0165-0173\(99\)00045-4](https://doi.org/10.1016/s0165-0173(99)00045-4)
 78. Zocchi A, Varnier G, Arban R, Griffante C, Zanetti L, Bettelini L, Marchi M, Gerrard PA et al (2003) Effects of antidepressant drugs and GR 205171, an neurokinin-1 (NK1) receptor antagonist, on the response in the forced swim test and on monoamine extracellular levels in the frontal cortex of the mouse. *Neurosci Lett* 345:73–76. [https://doi.org/10.1016/s0304-3940\(03\)00305-7](https://doi.org/10.1016/s0304-3940(03)00305-7)
 79. Li SX-M, Perry KW, Wong DT (2002) Influence of fluoxetine on the ability of bupropion to modulate extracellular dopamine and norepinephrine concentrations in three mesocorticolimbic areas of rats. *Neuropharmacology* 42:181–190. [https://doi.org/10.1016/S0028-3908\(01\)00160-5](https://doi.org/10.1016/S0028-3908(01)00160-5)
 80. D'Aquila PS, Collu M, Gessa GL, Serra G (2000) The role of dopamine in the mechanism of action of antidepressant drugs. *Eur J Pharmacol* 405:365–373. [https://doi.org/10.1016/s0014-2999\(00\)00566-5](https://doi.org/10.1016/s0014-2999(00)00566-5)

81. Kodl CT, Seaquist ER (2008) Cognitive dysfunction and diabetes mellitus. *Endocr Rev* 29:494–511. <https://doi.org/10.1210/er.2007-0034>
82. Yamagishi S, Nakamura K, Matsui T, Noda Y, Imaizumi T (2008) Receptor for advanced glycation end products (RAGE): a novel therapeutic target for diabetic vascular complication. *Curr Pharm Des* 14:487–495. <https://doi.org/10.2174/138161208783597416>
83. Szczepanik J, Garcia A, de Almeida G, et al (2020) Protective effects against memory impairment induced by methylglyoxal in mice co-treated with FPS-ZM1, an advanced glycation end products receptor antagonist. *Acta Neurobiol Exp (Wars)* In press:

Publisher's Note Springer Nature remains neutral with regard to jurisdictional claims in published maps and institutional affiliations.